PAPER

Check for updates

Morphologic alterations across three levels of biological organization following oral exposure to silver-polymer nanocomposites in Japanese medaka (*Oryzias latipes*)†

Melissa Chernick, [iD]*[a] Alan J. Kennedy,[c] Treye Thomas,[d] Keana C. K. Scott, [iD][f] Joana Marie Sipe, [iD][b] Christine Ogilvie Hendren, [iD][be] Mark R. Wiesner [iD][b] and David E. Hinton[a]

Polymer nanocomposites have diverse industrial and commercial uses. While many toxicity studies have assessed the individual materials (*e.g.*, polymer, nanomaterial) comprising nanocomposites, few have examined the potential toxicity of the nanocomposite as a whole. Furthermore, products undergo machining during their manufacture and/or degradation as they age thereby resulting in potentially altered mixture exposures and differential effects compared to the parent nanocomposite. We assessed potential toxic effects of repeated oral exposure to silver nanoparticle (AgNP) embedded nanocomposites and compared them to individual component materials using a transparent strain of the fish model Japanese medaka (*Oryzias latipes*). This strain allowed for the comparison of morphologic alterations at three levels of biological organization: whole animal; organ/tissue by examination of histologic sections; and, subcellular using transmission electron microscopy (TEM). Adult fish were exposed to AgNPs, silver nitrate, abraded PETG microplastics, or abraded nanocomposites *via* 7 oral gavages over the course of 2 weeks. *In vivo* observations showed alterations in the liver and gallbladder of fish exposed to pristine AgNPs and nanocomposites. When histologic sections of these same individuals were examined by light microscopy, hepatic and biliary alterations were observed. Similarly, alterations of the head kidney were also observed in fish exposed to silver and its composites, with both tubules and glomeruli affected. In both of these organs, many of the changes occurred adjacent to large blood vessels, suggesting material translocated from the bloodstream to adjacent tissues. TEM of the liver supported histological findings, with increased glycogen as well as hepatocellular swelling and abundant lipid vesicles in exposure groups. Very few morphological changes at any level of biological organization were observed in fish exposed to the plastic matrix alone. This transparent fish model proved advantageous in evaluating risks and potential human health concerns associated with the ingestion of silver nanocomposites.

Environmental significance

Nanocomposites are unique materials that enhance the already versatile characteristics of polymers by incorporating properties of nanomaterials. Recently, the widespread availability and use of these products by both consumers and manufacturers has raised concerns about potential exposure from particles released by this technology and over a product's lifetime. There is an abundance of environmental studies on silver nanoparticles and a continually growing body of literature on microplastics exposure yet there is a lack of toxicity studies on nanocomposites despite their increased use in various industries. Understanding of these unique mixtures is important in both an environmental context and from a human health perspective. Laboratory model fish, such as medaka, have been important for understanding this in the whole organism.

[a] *Nicholas School of the Environment, Duke University, 308 Research Drive, LSRC A341, Box 90328, Durham, NC, 27708, USA. E-mail: mc131@duke.edu; Tel: +1 (919) 613 8045*
[b] *Civil and Environmental Engineering, Duke University, Durham, NC, 27708, USA*
[c] *U.S. Army Engineer Research and Development Center, Environmental Laboratory, 3909 Halls Ferry Rd., Vicksburg, MS, USA*
[d] *United States Consumer Product Safety Commission, 4330 East-West Highway,*

Bethesda, Maryland 20814, USA
[e] *Department of Geological and Environmental Sciences, Appalachian State University, Boone, NC 28608, USA*
[f] *National Institute of Standards and Technology, 100 Bureau Drive, Gaithersburg, MD 20899, USA*
† Electronic supplementary information (ESI) available. See DOI: https://doi.org/10.1039/d4en00368c

This journal is © The Royal Society of Chemistry 2024

Environ. Sci.: Nano, 2024, **11**, 3317–3334 | **3317**

1. Introduction

Advanced materials (ADMAs) are innovative materials with novel or enhanced properties that improve their performance compared to conventional products.[1,2] The union of nanotechnology and polymer sciences has created a class unique materials with new properties dependent on the incorporated nanomaterials.[3] Nanomaterial incorporation leads to an improvement of the already useful properties of polymers including physical (*e.g.*, density, crystallinity), mechanical (*e.g.*, tensile strength), and biological (*e.g.*, antimicrobial, biodegradability) properties.[3,4] As a result, polymer nanocomposites have been used in numerous products including automobile parts, packaging, and biomedical supplies.[3,5]

The addition of nanomaterials to thermoplastics potentially changes the risks associated with it, leading to concerns about adverse health effects from particles released during fabrication and/or handling.[4,6,7] The discharge of ultrafine particles from manufacturing processes such as 3D printing and machining, or over the lifetime of a product, has the potential for occupational and residential exposure.[8,9] Safety standards have been set by agencies such as NIOSH (*e.g.*, Pelley[10]) for using 3D printers including some guidelines that include metals.[11] However, the toxicities of pristine nanomaterials or microplastics must be used as points of reference[4,12] as there are not many studies of the potential toxicities of specific nanocomposites.[4]

The enhanced antimicrobial properties of silver nanoparticles (AgNPs) make them attractive for use in a variety of medical and consumer product applications.[13] AgNPs also have physico-chemical properties such as high electrical and thermal conductivity, chemical stability, and catalytic activity that make them useful for various applications such as imaging and electronics.[14] Consequently, AgNPs are incorporated into a variety of polymers used in agriculture, medicine, textiles, and food packaging.[15,16]

In humans, ingestion is the primary exposure route for silver and silver compounds,[17] and studies have estimated daily uptake of 20 µg per day to 80 µg per day.[18,19] AgNPs leach from food and beverage packaging and from a variety of other consumer products (*e.g.*, plush toys, cleaning products, humidifiers) made of AgNP-enabled polymer nanocomposites.[20–24] During the manufacture of silver nanocomposite materials, occupational oral exposure may occur *via* swallowing after inhalation and expectoration when the affected individual attempts to clear materials from oral and nasal passageways (*i.e.*, phlegm).[19,25,26] Due to the absorptive nature of the gut and its proximity to various organs and tissues, toxic effects may occur at very low concentrations after oral or dietary exposure.[27] AgNPs are known to cross biological membranes such as the gut wall,[28] mainly by endocytosis in epithelial cells.[29] Studies using fish models have shown bioaccumulation in tissues such as gills, brain, and liver.[30,31] However, it is free silver ions (Ag^+) that are generally reported as toxic.[28] A Trojan horse effect could occur following exposure to AgNPs where Ag^+ is released inside tissues or cells.[32] Ag^+ is also released upon association of AgNPs with the surface of the cell's lipid plasma membrane as these ions are compatible for uptake by plasma membrane ion transporters.[29]

While there is an abundance of literature on the toxicity of AgNPs in multiple species, there are almost none on silver nanocomposites. This is concerning considering its increased use in a variety of fields (*e.g.*, medical, technology) and consumer products.[33] Nanomaterials released over a product's lifetime comprise only part of the equation for potential exposure and toxicity of nanocomposites. Particles released during machining (*e.g.*, abrading, cutting), environmental degradation and/or aging of products are largely composed of the polymer matrix[4,34–36] and, in the case of plastic nanocomposites, often in the form of microplastics (MPs).[37] Glycol-modified polyethylene terephthalate (PETG, $(C_{10}H_8O_4)_n$) is one such polymer widely used for applications such as 3D printing due to its transparency, higher thermal resistance, durability, and high elastic modulus.[38,39] Ingestion is also considered to be the major exposure route for MPs in humans.[40] Subsequently, particles can act locally and/or translocate to other tissues within the body.[40] Local effects have been shown in oral exposures using fish models, with various types of MPs altering gut morphology and negatively impacting intestinal health.[41–43] In turn, alterations in gut mucosa may increase permeability of epithelial barriers thereby facilitating translocation of particles, particularly to the liver and spleen.[40] In both instances, effects such as inflammation, cytotoxicity, and increased risk of neoplasia may result.[40] Because AgNPs are incorporated into plastics largely for their antimicrobial properties, biological effects of AgNP nanocomposites have predominately been studies of bacterial inhibition and cytotoxicity. There are very few investigations on the potential toxicity of these materials on non-target organisms, particularly higher taxa. Ours is one of the first studies that expand on the potential toxicity of nanocomposites, and specifically 3D printed nanocomposites, in a whole organism.

Fish models, such as the Japanese medaka (*Oryzias latipes*) used in this study, have been a valuable toxicological tool for the understanding of exposure in a whole organism.[44,45] In particular, they have been valuable predictive and experimental models in the study of disease formation and pathogenesis over relatively short time spans.[46] As such, there is extensive descriptive morphology and disease pathology available for multiple levels of biological organization.[47] Of interest for oral exposure in humans, are the similarities between teleost and mammalian digestive tracts including general architecture and processes of injury and inflammation.[48–50]

In this study, we used abraded PETG, pristine AgNPs, and abraded AgNP nanocomposites (two different nanoparticle loadings) that were created and fully characterized by Sipe *et al.*[51] The objective was to describe and assess morphologic

3318 | *Environ. Sci.: Nano*, 2024, **11**, 3317–3334

This journal is © The Royal Society of Chemistry 2024

alterations at multiple levels of biological organization associated with oral exposure in order to evaluate relative risks of released component materials compared to their composites. For this, we used a transparent strain of medaka to directly image acute morphologic changes to specific organs observed in the live animal and to compare them to tissue level alterations in histologic sections and cellular ultrastructure on an individual basis. Importantly, the small size of this species enabled whole body histologic sectioning so that multiple organs and tissues could be evaluated. Medaka also have a single lobed liver that facilitated clean removal and processing of the entire organ for transmission electron microscopy (TEM), avoiding issues of lobar distribution seen in some model organisms.[52] This was of interest because studies have shown AgNPs and microplastics to impact the liver.[53,54] In addition, our recent work demonstrated the liver as the organ most impacted by oral exposure to multi-walled carbon nanotube (MWCNT)-embedded nanocomposites.[55] Together, the investigation by Sipe et al.[51] in combination with our study are the first to evaluate the mechanical breakdown of silver nanocomposites and their potential toxicity in a vertebrate.

2. Materials and methods

2.1. Materials

In depth descriptions and characterizations of the materials used in this study are detailed in Sipe et al.[51] Briefly, AgNPs were uncoated, spherical silver nanoparticles purchased from NanoDynamics, Inc. (ND30, Buffalo, NY) with a reported size of 30 nm. A Mastersizer 3000 laser diffractometer (Malvern,

UK) in batch mode (1 g L^{-1}) was used to measure particle size distribution. AgNPs had a diameter ranging between 20 nm and 50 nm. Zeta potential was measured using the Nanosizer NanoZS (Malvern Panalytical Ltd.). AgNPs were negatively charged, with a zeta potential of −19 mV ± 3 in distilled water, −20 mV ± 6 in freshwater (pH 7.4), and 4 mV ± 10 in artificial saltwater (pH 8.4). A typical TEM image of these pristine AgNPs is shown in Fig. S1.†

Neat PETG filament and AgNP-polymer nanocomposite filaments were prepared from virgin filament grade PETG polymer pellets (ChasePlastics, Clarkston, MI) and AgNPs. Mass fractions of AgNPs in nanocomposite filaments were either 2% or 0.5%. First, filaments were made by mixing PETG matrix pellets with the powdered AgNPs. Then these mixtures were extruded (Eurolab XL 16 twin-screw extruder) three times to ensure even mixture of the nanoparticles with the polymer matrix. Neat and nanocomposite PETG filaments were 3D printed into cylinder pucks (diameter of 50.8 mm and thickness of 5 mm; printer settings in ESI†). PETG matrix and nanocomposite materials were abraded as described below to simulate wear and degradation during of a product during its lifecycle. Hereafter, the abraded neat PETG matrix will be referred to as PETG, pristine AgNPs as AgNPs, and abraded nanocomposites as either 2% composite or 0.5% composite.

An abrasion machine designed and custom built at Duke University as described by Bossa et al.,[37] Sipe et al.,[56] and Scott et al.[57] was used to create abraded polymer and nanocomposite materials for this study (Fig. 1). The machine included a spinning abrasion platform with P100 sandpaper that was able to maintain a constant abrasion with the same

Fig. 1 Light micrographs showing abraded polymer (A and D) and 2% (B and E) and 0.5% (C and F) nanocomposite materials. Low magnification of materials are along the top row (A–C, scale bars 100 μm) and high magnification of each of those materials is along the bottom row (D–F, scale bars 20 μm). A and D) Abraded pristine PETG plastic; B and E) 2% AgNP nanocomposite; and C and F) 0.5% AgNP nanocomposite. Arrows point to AgNPs aggregates (dark dots) on or within PETG matrix.

This journal is © The Royal Society of Chemistry 2024

Environ. Sci.: Nano, 2024, 11, 3317–3334 | 3319

power and abrasion rate. An airtight chamber enclosed the sample holder and allowed for collection of particles generated during the abrasion process. The full characterization of these particles is also detailed in Sipe *et al.*[51] The presence of AgNPs within a composite did not affect the abrasion process, but although each puck underwent the same abrasion process, the presence and concentration of AgNPs affected the resulting wear particle size (Mastersizer 3000). The D50 particle size (*i.e.*, mean diameter of 50% of particles) by volume was 695.5 μm ± 230.8, 39.8 μm ± 0.2, and 143.8 μm ± 4.4 for PETG, 0.5% composite, and 2% composite, respectively. SEM with EDS imaging confirmed the presence of AgNPs on and in abraded nanocomposite particles. Zeta potentials of PETG, 0.5% composite, and 2% composite were −33 mV, −21 mV, and −17 mV, respectively, in distilled water. Zeta potentials were within a standard deviation of each other, signifying that the incorporated AgNPs (free or at the surface) did not affect their behavior in water. It should be noted that at neutral pH, elemental silver has very little solubility and at pH values greater than of 8, approximately 80% of any dissolved silver precipitates as silver oxide or silver sulfide.[58] The exact pH of the gut of agastric fishes is difficult to determine and data are often highly variable.[59] There is some recent work in zebrafish, a very similar fish model to medaka, that indicates that gut pH is likely above 7.5.[60]

Dissolution of silver for each of the materials was determined at two time points, 1 h and 24 h. These time points were selected to represent the times after solution preparation for which the fish was dosed (1 h) and the maximum amount of time that the material likely stayed within the gut before egestion (24 h). All solutions were prepared in MilliQ water (ddH$_2$O; EMD Millipore, Burlington, MA) in triplicate using the same methods and concentrations that would be used for dosing fish (section 2.3). Next, each solution was allowed to sit at room temperature in the dark for either 1 h or 24 h. After the allotted time, all samples including procedural controls were filtered using a 0.2 μm cellulose acetate membrane syringe filter (VWR International, Radnor, PA). Then 0.5% trace metal grade nitric acid (HNO$_3$; Millipore Sigma) and 0.5% trace metal grade hydrochloric acid (HCl; Millipore Sigma) were added to each. Samples were than quantified for silver concentration (μg L^{-1}) by inductively coupled plasma-mass spectrometry (ICP-MS; Agilent 7700X ICP-MS equipped with an Octopole Reaction System) in the Pratt School of Engineering at Duke University (Durham, NC) using hydrogen reaction gas at a H$_2$(g) flow rate of 6 mL min^{-1} with a silver NIST standard. Results of this test can be found in Table S1.†

2.2. Medaka culture

Transparent, Quintet mutant strain medaka (Strain ID: MT829; Sasado *et al.*[61]) were maintained at Duke University in a recirculating system (pentair Aquatic Eco-Systems, Apopka, FL) at 24 °C, with a pH 7.4 and a 14:10 light:dark

cycle. Colony fish were fed three times per day with Otohime β1 commercial dry diet (200 μm to 360 μm, penta-ir Aquatic Eco-Systems). The first two feedings were supplemented with *Artemia* nauplii (90% Great Lakes Strain, pentair Aquatic Eco-Systems). All animal procedures were performed in accordance with the Guidelines for Care and Use of Laboratory Animals of Duke University and approved by the Animal Ethics Committee of the Institutional Animal Care and Use Committee (protocol no: A062-15-02 and A031-15-01).

2.3. Exposure regime

AgNP solutions were made fresh just prior to each dosing. For this, a stock solution was prepared by placing 1 mg AgNP powder into 100 mL autoclaved ddH$_2$O. Next, this stock solution was sonicated (80% pulse; BioLogics Inc. 3000 ultrasonic homogenizer, Manassas, MA) for 30 minutes on ice to disperse particles. Immediately following sonication, the solution was diluted with autoclaved ddH$_2$O to the test concentration and immediately administered to fish as described below. All abraded materials were suspended in autoclaved ddH$_2$O and vortexed to distribute particles just prior to administration to each fish. A preliminary range-finding assay using 3 doses of AgNPs was completed. From these data, 1000 μg L^{-1} AgNPs was selected as the test concentration. This concentration is consistent with consumer product leaching data, specifically the high AgNP release in media similar to that which we used (*i.e.*, water and saliva).[23] We also took into consideration concentrations used in three studies that tested chronic or repeated dietary AgNP exposure in adult fish. Lacave *et al.*[62] exposed zebrafish (*Danio rerio*) to 100 μg L^{-1} of 5 nm polyvinyl pyrrolidone/polyethylenimine (PVP/PEI)-coated AgNPs *via Artemia* spp. nauplii for 21 days. Merrifield *et al.*[63] fed zebrafish diet spiked with 500 mg kg^{-1} of uncoated 59 nm AgNPs for 14 days. Wang and Wang[64] exposed marine medaka (*Oryzias melastigma*) to 200 μg L^{-1} or 1000 μg L^{-1} of 20 nm AgNPs stabilized with Tween20 (0.025 g mol^{-1} or 20 μM) *via Artemia* spp. nauplii for 28 days.

For comparison, doses of abraded materials (PETG, 2% composite, 0.5% composite) were calculated to achieve the same AgNP mass dose of 1000 μg L^{-1}. AgNO$_3$ was tested at 65% of the concentration of AgNPs to account for silver ions (Ag$^+$).[65–67] Concentrations (μg L^{-1}) of all materials were: 1000 AgNPs; 650 AgNO$_3$; 49 000 PETG; 50 000 2% composite; or 200 000 0.5% composite.

Adult fish (8 mo. old) were selected from the colony and briefly examined to ensure there were no gross internal abnormalities. Five fish (3 females, 2 males) per group were randomly divided into 7.5 L glass aquaria in a dedicated room at 24 °C and a 14:10 light:dark cycle. Aquaria contained batch water consisting of 1 g L^{-1} of aquarium salt (Instant Ocean, Blacksburg, VA) in reverse osmosis (RO) treated water that was mixed and oxygenated for at least 16 h before use. Each aquarium was equipped with independent

3320 | *Environ. Sci.: Nano*, 2024, **11**, 3317–3334

This journal is © The Royal Society of Chemistry 2024

heaters for temperature control, pumps for mechanical filtration, and ceramic beads taken from the colony system for biological filtration (Fig. S2†). Aquaria were siphoned twice daily to remove fish waste, eggs, and uneaten food. Filters were rinsed with DI water once per day and changed for new every 3 days. Water quality (e.g., temperature, pH, ammonia, nitrite, nitrate) was tested daily with an API Freshwater Master Test Kit and 30% water changes conducted once per week or as needed to maintain stable water quality. Each experimental group had dedicated instruments (nets, siphons, etc.) to prevent cross-contamination. Fish remained on the breeding colony feeding regime (section 2.2) during their 3-day acclimation period.

Experimental fish were administered material every other day for 14 days, resulting in a total of 7 doses. Procedural controls received the suspension media (i.e., autoclaved ddH$_2$O) only. Fish were fasted for 24 h prior to each dose to clear the gut of digestate, and then doses were administered using oral gavage as a method to deliver precise quantities of material to the digestive tract of each individual. Methods for oral gavage followed exactly those detailed by Chernick et al.[55] In short, individual fish were anesthetized by submersion in 0.024% MS-222 (pentair Aquatic Eco-systems), pH 7.4, and then carefully placed into a trough cut into a soft sponge (L800-D, Jaece Industries, North Tonawanda, NY) moistened with batch water such that the head faced up and opercular movement was not obstructed. Next, a 13 mm length of micro-renathane catheter tubing (MRE-025, Braintree Scientific, Inc., Braintree, MA) was placed over a 31G, 8 mm needle of a sterile syringe (BD Biosciences, San Jose, CA) such that approximately 5 mm extended past the end of the needle and 10 μL of dosing solution was drawn up into the tubing. Tubing was gently inserted into the oropharynx, just caudal to the branchial chamber. Material was injected slowly and then the tubing removed. Fish were constantly monitored for normal opercular movements and gill color, heart rate, and responsiveness. Following oral gavage, each fish was rapidly examined for obvious internal alterations (e.g., hemorrhaging, gallbladder color change, enlargement/darkening of liver) and then placed into a large bowl containing batch water where it was monitored for recovery and possible regurgitation. Following recovery from anesthesia, the fish was returned to its original tank and the procedure repeated with the next individual.

Twenty-four hours after the last dose, fish were euthanized with an overdose of MS-222 (300 mg L^{-1}; Pentair Aquatic Ecosystems) and then digitally photographed (Olympus Corp., Center Valley, PA) in both lateral and dorsal recumbency. The latter was facilitated by placing the fish in the same type of sponge used for gavage. During this time, in vivo alterations were recorded as both descriptions and presence/absence data. These observations were later verified in images. Fish were then either fixed for histology (section 2.4) or livers were dissected and fixed for cellular ultrastructure (section 2.5). Specimens, liver and whole animals, were stored in individually labeled containers so that results from each could be compared to in vivo images on an individual basis.

2.4. Histology

Four fish (2 females, 2 males) in each group were fixed for histology immediately after imaging and for in vivo evaluation according to Chernick et al.[55] In brief, to facilitate fixation of deep tissues, a ventral incision was made from the anus to near the pectoral girdle. Then 10% neutral buffered formalin (10% NBF; VWR International) was very gently flushed into the incision, making sure not to displace internal organs. Next, 10% NBF was flushed into the buccal cavity such that it could enter the branchial cavity, pharynx and foregut. Finally, each fish was immersed in 10 times their volume of 10% NBF, placed on an orbital shaker (≈5.2 rad s^{-1} or 50 rpm) overnight, and then stored at 4 °C until processing. Prior to processing, specimens were brought to room temperature, the tail removed just caudal to the abdomen using a single edged razor blade, and the specimen submerged in fresh 10% NBF.

These fish were processed, embedded, sectioned, and stained by the Histology Laboratory, Department of Population, Health and Pathobiology, College of Veterinary Medicine, North Carolina State University, Raleigh, NC. First, fish were decalcified by placement in 10% formic acid for 48 h. Next, they were placed in an automated tissue processor (Thermo Shandon Path Centre, Grand Island, NY) and dehydrated by passage through a graded ethanol (EtOH) series and then cleared with Clear-Rite 3 (Richard Allen Scientific, Kalamazoo, MI). Processed fish, in right lateral recumbency, were individually embedded in paraffin. Parasagittal sections were cut at 5 μm thickness using a Leica 2135 rotary microtome (Leica Biosystems Inc., Buffalo Grove, IL) and then mounted on glass histology slides. Slides were routinely stained with hematoxylin and eosin (H&E) and coverslipped.

All labeling of slides were covered to ensure sections were examined blindly. Examination took place using a Nikon Alphaphot II compound light microscope. The presence or absence of various alterations (Table 1) was recorded for each individual and calculated as proportion of individuals within a group showing a change. Definitions for each of the categories of change followed those published in ESI† in Chernick et al.[55] In this way, relative occurrences of each alteration were established in each treatment group. Representative images were taken using a Nikon E600 compound light microscope fitted with a Nikon DXM1200 digital camera and Nikon NIS-Elements 3.10 software (Nikon Instruments Inc., Melville, NY).

2.5. Transmission electron microscopy

Reagents and consumables were purchased from Electron Microscopy Sciences (EMS; Hatfield, PA). All stains were filtered (syringe filter, nylon, 0.2 μm, VWR International) prior to use so that stain particulates would not be confused

This journal is © The Royal Society of Chemistry 2024

Environ. Sci.: Nano, 2024, 11, 3317–3334 | 3321

Table 1 Proportions of individuals in each experimental group affected with various types of changes as observed in histologic sections. Indents indicate subcategories of alterations within an organ or tissue and superscripted letters designate statistical differences between groups

	Control	PETG	AgNO$_3$	AgNPs	2% composite	0.5% composite
Gut alterations	0	50	75^{a,e}	100^{a,e}	50	0
Increased mucus	0	0	75^{a,b,d,f}	0	25	0
Alteration on apex of gut folds	0	50	75^{a,e}	100^{a,e,f}	25	0
Branchial alterations	100	75	100	66.7	100	75
Swollen opercular epithelium	75	50	100	66.7	75	75
Epithelial lifting of lamellae	0	50	50	66.7	100^{a,b}	75^{a,b}
Altered opercular epithelial cells	75	25	25	66.7	100^{b,c}	75
Liver alterations	0	50	75^{a,b}	100^{a,b}	100^{a,b}	100^{a,b}
Hepatocellular alterations	0	25	75^a	100^{a,b}	100^{a,b}	100^{a,b}
Hepatocellular swelling	0	25	75^a	100^{a,b}	100^{a,b}	100^{a,b}
Hepatocellular shrinkage	0	0	0	0	100^{a,b}	100^{a,b}
Vacuolated hepatocytes	0	0	25	0	50	0
Pyknotic nuclei in hepatocytes	0	25	0	66.7	25	25
Necrotic hepatocytes	0	0	25	100^{a,b,c,e,f}	25	25
Spongiosis hepatis	0	0	0	0	0	75^{a,b,c,d,e}
Perivascular fluid accumulation	0	25	0	66.7	25	25
Biliary alterations	0	25	75^a	33.3	50	100^{a,b}
Altered biliary epithelial cells	0	0	0	0	0	50
Reactions adjacent to biliary structures	0	0	50	33.3	25	25
Peribiliary fluid accumulation	0	25	50	0	50	25
Vascular congestion	0	0	0	0	0	100^{a,b,c,d,e}
Altered head kidney	0	100^a	75^a	100^a	100^a	100^a
Altered tubules	0	100^a	75^a	100^a	100	100
Altered tubular epithelial cells	0	50	75^a	100^a	75^a	100^a
Dilated tubules	0	25	0	33.3	50	25
Increased tubulogenesis	0	25	50	33.3	50	50
Altered glomeruli	0	25	75^a	100^{a,b}	100^{a,b}	100^{a,b}
Shrunken glomeruli	0	0	0	33.3	50	25
Congested glomeruli	0	0	0	33.3	0	100^{a,b,c,e}
Calcifications in glomeruli	0	0	25	0	0	50
Eosinophilic material in glomeruli	0	25	50	66.7	25	50
Altered Bowman's capsule	0	25	25	33.3	75^a	75^a
Increased glomerulogenesis	0	50	0	0	50	25
Altered trunk kidney	0	25	75^{a,e}	33.3	0	25
Altered oval body	0	0	75^{a,b,d,e}	33.3	0	0
Vacuolated cells	0	0	50	0	0	0
Swollen cells	0	0	50	0	0	0
Injured cells	0	0	25	33.3	0	0
Inflammation	0	25	50	100^{a,b}	100^{a,b}	75^a
Inflammation on serosal surface	0	0	0	100^{a,b,c}	75^{a,b,c}	25^d
Inflammation in liver	0	25	50	66.7	100^{a,b}	75^a
Macrophage aggregates	0	25	0	33.3	0	0
Perivascular inflammation	0	0	25	66.7	50	75^{a,b}
Peribiliary inflammation	0	0	50	66.7	100^{a,b}	75^{a,b}

$p \leq 0.05$. ^{a} Compared to control. ^{b} Compared to PETG. ^{c} Compared to AgNO$_3$. ^{d} Compared to AgNPs. ^{e} Compared to 2% composite. ^{f} Compared to 0.5% composite.

with AgNPs. Specimen preparation and processing followed Chernick *et al.*[55] For each group, a single female fish was imaged as described above and observations under *in vivo* evaluation recorded. Dissected livers were then immediately placed into 2.5% glutaraldehyde buffered with a cacodylate-sucrose solution (0.1 mol L^{-1} sodium cacodylate and 0.1 mol L^{-1} sucrose, pH 7.6) and fixed at 4 °C. Just prior to processing, each liver was cut into 4 or 5 relatively equal sized pieces using a single-edged razor blade and each piece was placed in a labeled 20 mL borosilicate glass vial (Wheaton, VWR International). After washing twice in 1X PBS (10 min per wash), specimens were stained with 1% osmium tetroxide (OsO$_4$) in the dark for 1 hour. Then samples were

again washed with 1x PBS and rinsed with acetate buffer (10.17 g mol^{-1} (124.43 mM) sodium acetate, 1.5 g mol^{-1} (25 mM) acetic acid) before staining with 0.5% uranyl acetate for 1 hour. Next, specimens were rinsed with acetate buffer and dehydrated by passage through a graded EtOH series. Samples were then placed in propylene oxide (PO) three times for 10 min each. Spurr's resin was prepared (16.4 g cycloaliphatic epoxide resin (ERL-4221), 23.6 g nonenyl succinic anhydride (NSA), 5.72 g Dow epoxy resin (DER 736), 0.4 g 2-dimethylaminoethanol (DMAE)), and samples were immersed in a Spurr's : PO (1 : 2) mixture in a chemical fume hood for 4 hours with the vial caps off and then overnight with the caps on. The next day, the mixture was replaced with

a Spurr's:PO (1:1) mixture and cured for 8 hours in a chemical fume hood with vial caps off. This mixture was then replaced twice with new, pure resin and incubated in a 60 °C oven for at least 10 minutes each time. For embedding, fresh resin was placed in a flat multi-well embedding mold with liver portions positioned near the tips and were allowed to cure in a 60 °C oven for 24 hours. These blocks were thin sectioned at 70 nm to 90 nm thickness, placed on 150 square mesh copper gilder grids (#G150-CU, EMS), and then stained with lead citrate. Thin sections were examined and imaged at 80 kV using a FEI Tecnai G^2 Twin transmission electron microscope with a single tilt stage, and a spot size of 2.

2.6. Data analysis

Morphologic alterations were recorded as presence/absence data for *in vivo* (*i.e.*, whole animal) and in histology (Table 1; $n = 4$). For these data, Pearson Chi-squared pairwise tests were conducted using the categorical response analysis tool in JMP Pro 14 (SAS Institute, Cary, NC) comparing incidence of individual changes between experimental groups. For clarity, statistical differences and associated *p*-values described within the text of section 3 (Results) are comparisons to control fish. Percentages reported herein represent incidences of fish within a group with the alteration. A full comparison, including proportions of affected fish and any statistical differences between other treatment groups, for histological alterations can be found in Table 1. *P*-Values of ≤0.05 were considered to be statistically significant.

3. Results

3.1. *In vivo* observations

An incidental single mortality of a male fish occurred in the 1000 μg L^{-1} AgNP group on day 4 (after 2 doses). No other
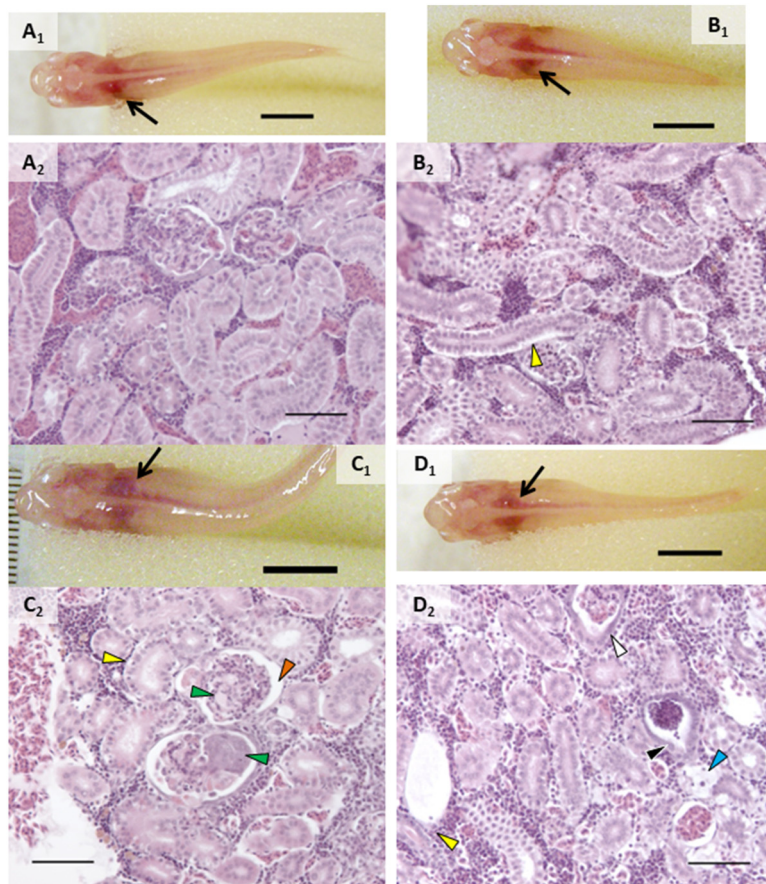

Fig. 2 Representative images of alterations observed in head kidney *in vivo* and in histologic sections on an individual basis. A) Control fish with normal kidney observed *in vivo* (A$_1$) and head kidney with normal tubules and glomeruli in histologic sections of that same individual (A$_2$); B) fish exposed to AgNO$_3$ showed no alterations *in vivo* (B$_1$) but had increased intercellular spaces between tubular epithelial cells (B$_2$, yellow arrowhead); C) head kidney of fish exposed to AgNPs with lighter appearance *in vivo* (C$_1$) had increased intercellular spaces between tubular epithelial cells (yellow arrowhead), increased Bowman's space (orange arrowhead), and glomerular congestion and necrosis (green arrowheads) in histologic sections (C$_2$); D) fish exposed to 0.5% composite appeared to have normal kidney when observed *in vivo* (D$_1$) but had increased intercellular spaces between tubular epithelial cells (yellow arrowhead) and thickening of tubular epithelium within the vascular layer (black arrowhead), tubular degeneration (blue arrowhead) when assessed in histologic sections. *In vivo* scale bars (A$_1$–D$_1$) are 5 mm and black arrows point to head kidney. Histology scale bars (A$_2$–D$_2$) are 50 μm.

This journal is © The Royal Society of Chemistry 2024

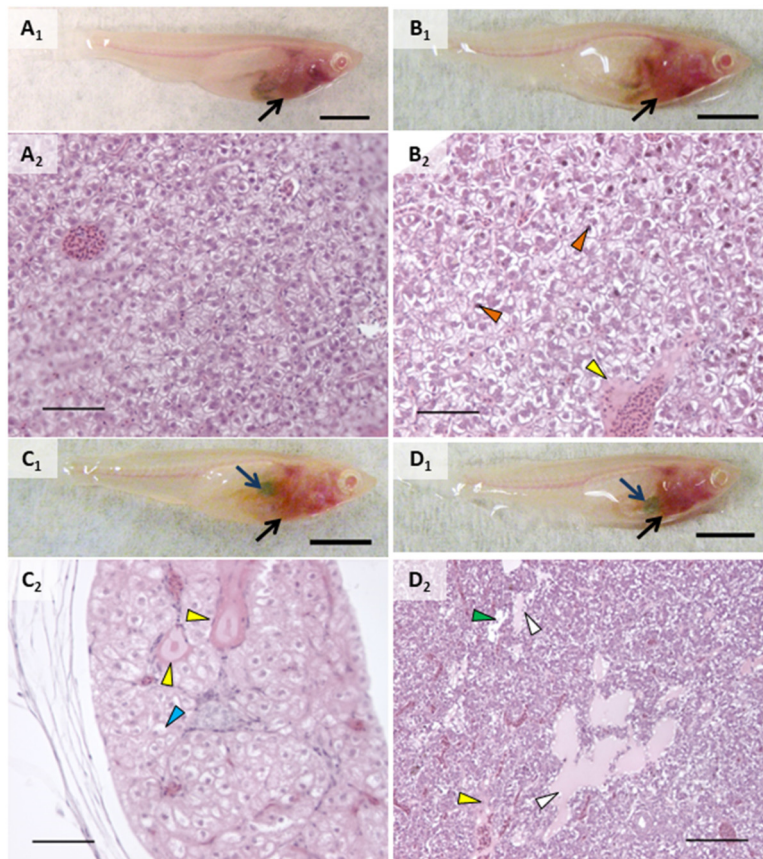*Environ. Sci.: Nano*, 2024, **11**, 3317–3334 | **3323**

Fig. 3 Representative images of alterations observed in liver *in vivo* and in histologic sections on an individual basis. A) Control fish with normal liver observed *in vivo* (A_1, black arrow) along with normal liver parenchyma in histologic sections (A_2) of that same individual; B) fish exposed to $AgNO_3$ showing normal liver when observed *in vivo* (B_1, black arrow) but pyknotic nuclei (orange arrowheads) and perivascular fluid accumulation (yellow arrowhead) in histologic sections (B_2); C) fish exposed to AgNPs showing liver discoloration (black arrow) and enlarged and darkened gallbladder (blue arrow) *in vivo* (C_1) and perivascular fluid (yellow arrowheads) and widespread hepatocellular swelling (blue arrowhead) in sections (C_2); D) fish exposed to 2% composite showing lightening of the caudal portion of the liver (black arrow) nearest a darkened and enlarged gallbladder (blue arrow) *in vivo* (D_1), with histologic sections showing peribiliary fluid accumulation (white arrowheads), perivascular fluid (yellow arrowhead), and hepatocellular swelling (blue arrowhead). Scale bars on *in vivo* images (A_1–D_1) are 5 mm. Scale bars on histologic sections are 100 μm (A_2–C_2) and 50 μm (D_2).
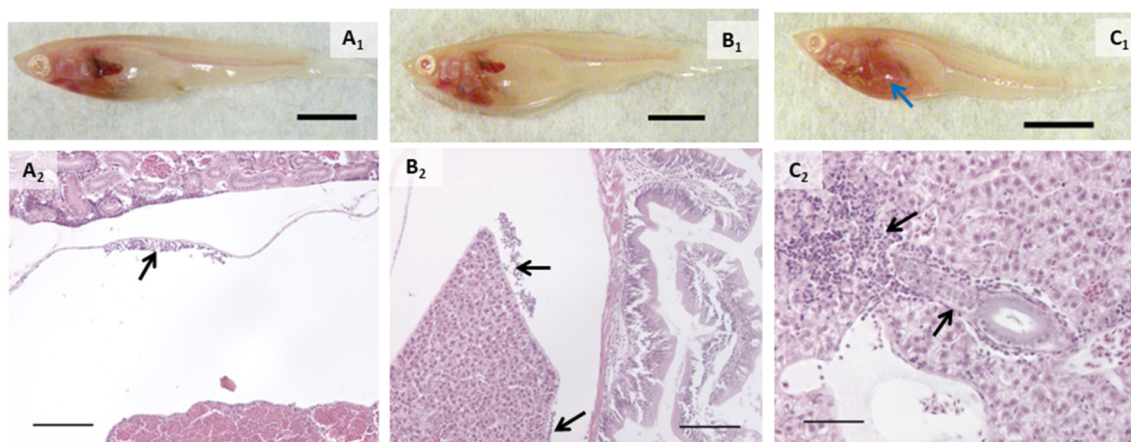

Fig. 4 Examples of inflammation in exposed fish. Top row are *in vivo* images of fish with the bottom row showing histologic sections of these same individuals. A) Abdominal cavity from fish exposed to $AgNO_3$ showing accumulation of macrophages (A_2); B) abdominal cavity from fish exposed to AgNPs showing accumulation of macrophages between the liver and gut; C) liver from a fish exposed to 2% composite showing inflammation around biliary passageways and blood vessels (C_2). Blue arrow (C_1) points to liver, and black arrows point to inflammation (C_2). Scale bars on *in vivo* images (A_1–C_1) are 5 mm. Scale bars on histologic sections are 100 μm (A_2, B_2) and 50 μm (C_2).

3324 | *Environ. Sci.: Nano*, 2024, **11**, 3317–3334

This journal is © The Royal Society of Chemistry 2024

mortalities or behavior that would suggest stress (*e.g.*, cowering, gasping) were observed in other fish during the experiment including prior to mortality in the single male fish. Fish were not observed to regurgitate gavaged material upon recovery from anesthesia.

In vivo assessment showed that control fish had no alterations and exposed fish had a few types of alterations (Fig. 2–4). Discoloration, specifically lightened patches, of the head kidney was observed following exposure to AgNPs but not in a significant number of individuals (Fig. $2C_1$). Enlargement and/or discoloration (*i.e.*, darkened or mottled appearance) of the liver was observed in 75% of fish exposed to AgNPs (Fig. $3C_1$) and 60% of fish exposed to 2% composite (Fig. $3D_1$) ($p = 0.0177$ and 0.0384, respectively). It should be noted that had the other male survived in the AgNP group and had a normal liver, this group would still have had a statistically significant difference. Gallbladder alterations (*i.e.*, darkened or altered color and/or enlargement) were not observed until after the sixth dose in any group and persisted until after the final dose (Fig. 3). The 2% composite group had significantly more fish with this change than the control group ($p = 0.0098$, Fig. $3D_1$) and the 0.5% composite group ($p = 0.0384$). Half of the fish in the AgNP group had this change (Fig. $3C_1$), which was not statistically significant. Changes in the midgut (*i.e.*, large clear areas around a bolus, indicating distention or discoloration of walls), or fluid accumulation in the peritoneal cavity, were not observed in any fish.

3.2. Histologic evaluation

Proportions of individuals affected with various types of change are listed in Table 1. Alterations within the branchial chamber were observed within all groups including control, which may have been the result of anesthesia or the gavage procedure. While the exposure route was dietary, epithelial lifting on primary and secondary lamellae in some groups suggested a small amount of silver may have interacted with gill tissue. AgNO$_3$ and AgNPs caused damage to apical cells of the mucosal gut folds ($p = 0.0285$ and 0.0082, respectively). The oval body of the swim bladder was significantly affected in fish exposed to AgNO$_3$ ($p = 0.0285$), with vacuolated, swollen, and injured cells observed. While not statistically significant, it is worth noting that the only other treatment group that had any incidence of this change was AgNPs, with injured cells in the swim bladder.

The head kidneys showed a variety of changes in exposed fish of each treatment group (Fig. 2, Table 1). Tubules were altered in all groups except control ($p < 0.05$; Fig. 2). Tubule alterations included altered tubular epithelial cells, dilated lamina of tubules, and increased tubulogenesis. Alterations in tubular epithelial cells were characterized by increased intercellular spaces, intermittent degeneration or damage, and loss of contact with the basement membrane (Fig. 2). The proportion of individuals with this change was higher after exposure to AgNO$_3$ ($p = 0.0285$), AgNPs ($p = 0.0082$), 2%

composite ($p = 0.0285$), and 0.5% composite ($p = 0.0047$). It is noteworthy that the proportion of fish with altered tubules was the only statistically significant change for fish exposed to PETG. Dilated tubules were typically adjacent to large veins within the head kidney and occurred in all groups except control and AgNO$_3$ but incidence was not statistically significant ($p > 0.05$). Calcifications in the tubule lumens were observed in fish exposed to PETG ($p = 0.0136$) but were small and infrequent. When encountered, alterations in the trunk kidney were infrequent and minor. However, these alterations occurred in more fish exposed to AgNO$_3$ ($p = 0.0285$).

Altered glomeruli were observed in fish exposed to AgNO$_3$ ($p = 0.0285$), AgNPs ($p = 0.0082$), 2% composite ($p = 0.0047$), and 0.5% composite ($p = 0.0047$). Alterations within the glomerular tuft included congestion of capillaries, calcifications, an abundance of eosinophilic material, altered Bowman's capsule, and/or necrosis of glomerular cells (Fig. $2C_2$, Table 1). Except for congestion, there were no statistical differences between treatment groups when these individual types of changes were analyzed independently. All fish exposed to 0.5% composite had congestion in the capillaries of the glomeruli ($p = 0.0047$). The only other group to have this change was AgNPs (33.3%) although it was not statistically significant. Alterations in Bowman's capsule were characterized by basophilic epithelium within the visceral layer (*i.e.*, podocytes) and/or changes in Bowman's space that included expansion or reduction and instances of fibrous material that extended through the space (Fig. $2C_2$ and D_2). The latter change is an unusual finding that only occurred in fish in composite groups (1 fish in each). The number of fish that had alterations in Bowman's capsule was significantly higher in the 2% composite and 0.5% composite groups ($p = 0.0285$ in both groups).

When grouping all types of liver alterations together, both hepatocellular and biliary, fish exposed to silver and composites were most affected. Fish in the PETG group were more similar to controls. While a couple of the PETG exposed fish had either perivascular or peribiliary fluid accumulation, it was minor, and they exhibited very few other liver changes. 75% of fish exposed to AgNO$_3$ had liver alterations ($p = 0.0285$) while all fish exposed to AgNPs and composites had liver alterations ($p = 0.0047$). Hepatocellular alterations included swelling and shrinking, vacuolated hepatocytes, pyknotic nuclei, necrosis, spongiosis hepatis, and/or perivascular fluid accumulation (Fig. 3, Table 1). Several of these changes often occurred within the same individual. Hepatocellular swelling was, by far, the most extensive change both in terms of extent/severity within individuals and proportion of fish affected within treatment groups. Swollen hepatocytes had rounded or irregular margins, and a majority of the cytoplasm showed little staining or staining was restricted to a perinuclear region (Fig. $3B_2$ and C_2). 75% of fish in the AgNO$_3$ group had this change ($p = 0.0285$) as well as all fish exposed to AgNPs, 2% composite, or 0.5%

This journal is © The Royal Society of Chemistry 2024

Environ. Sci.: Nano, 2024, **11**, 3317–3334 | **3325**

composite (p = 0.0082, 0.0047, and 0.0047, respectively). Areas of altered livers exhibited shrunken hepatocytes, often with pyknotic nuclei, typically in the region closest to the foregut and porta hepatis (Fig. 3B$_2$). Interestingly, shrunken hepatocytes only occurred in fish exposed to composites, and to all fish of these treatment groups (p = 0.0047). For half of the individuals in the 2% composite group, the overall size of the liver appeared slightly to moderately larger, likely a result of these changes in cell volume (Fig. S3B†). Scattered necrotic hepatocytes were observed in all treatment groups except for control and PETG; all fish exposed to AgNPs had necrotic hepatocytes. Spongiosis hepatis was found in fish exposed to 0.5% composite (75%, p = 0.0285). This alteration was characterized by hepatocyte swelling such that cells became very large with nuclei displaced to the periphery by fluid and/or protein-like material, forming lesions with sharp margins. This alteration may have given the liver a mottled or lighter appearance in these individuals *in vivo*.

Biliary alterations included reactions around biliary structures, alterations of biliary epithelial cells, and/or peribiliary fluid accumulation (Fig. 3D$_2$, Table 1). Fish in the AgNO$_3$ and 0.5% composite groups had more instances of

these alterations (p = 0.0285 and 0.0047, respectively; Fig. 3). However, individual types of biliary responses did not show significant differences (Table 1). That said, it is notable that only fish in the 0.5% composite had alterations of biliary epithelial cells. All groups containing silver had at least one individual that showed reactions adjacent to or within biliary structures. While no statistical differences were found in incidence of peribiliary fluid accumulation, it is notable that the AgNP group was the only one apart from the control that did not have this change.

Inflammation was another major finding of this experiment and appeared to primarily be the result of AgNP exposure, both in its pristine form as well as that associated with composites. For the purposes of our analysis, we defined "inflammation" as a cellular response (*i.e.*, white blood cells) because humoral components of the immune system are not visible in histologic sections. An inflammatory response was observed in fish exposed to PETG or AgNO$_3$, but it was minor, and the number of individuals with it was not significantly different from control. Inflammation was found in more fish exposed to AgNPs (p = 0.0082, Fig. 4B$_2$), 2% composite (p = 0.0047, Fig. 4C$_2$), and 0.5% composite (p = 0.0285). When

Fig. 5 TEM micrographs of livers from female medaka 24 hours after final dose. A) Control liver had normal hepatocytes with narrow intercellular spaces, rough endoplasmic reticulum (RER) with parallel cisternae and narrow cisternal spaces, few secondary lysosomes, and some lipid droplets; B) liver from medaka exposed to pristine PETG was like that of control except for large areas containing glycogen; C) liver of individual exposed to AgNO$_3$ was like that of the control except for moderately sized areas containing glycogen; D) liver of individual exposed to AgNPs showed glycogen to be spread out and plasma membranes were indistinct, suggesting hepatocellular swelling; E and F) liver from fish exposed to 2% (E) or 0.5% (F) abraded composites closely resembled each other and control, with some increased glycogen. Arrowheads: purple – intercellular spaces, blue – secondary lysosomes, orange – hepatocyte nucleus, green – glycogen, red – RER, white - peribiliary structure/space, yellow – lipid, black – biliary epithelial cell, white arrow – macrophage. A, D and E at 1700× magnification with 2 μm scale bars and B and F at 3500× magnification with 1 μm scale bars.

3326 | *Environ. Sci.: Nano*, 2024, **11**, 3317–3334

This journal is © The Royal Society of Chemistry 2024

looking at specific locales of inflammation, some patterns emerged. More fish in the 2% composite (p = 0.0047, Fig. 4C$_2$) and 0.5% composite (p = 0.0285) groups had inflammation within the liver, either perivascularly or peribiliary (p = 0.0047 and 0.0285 for 2% composite and 0.5% composite, respectively). Macrophage aggregates were present in a small number of fish exposed to AgNPs and were generally small in size ($\leq$200 μm) and extent. Inflammation also occurred within the mesentery, specifically on the serosal surface of the gut and margins of the liver (Fig. 4A$_2$ and B$_2$). This only occurred in groups exposed to silver, with all fish in the AgNP group (p = 0.0082) and 75% of fish in the 2% composite group (p = 0.0285) having this response.

3.3. Liver ultrastructure

TEM of liver from the control fish (Fig. 5A) had normal structure, with uniform hepatocytes, each with a single nucleus containing a defined nucleolus; rough endoplasmic reticulum (RER) with straight parallel cisternae with narrow cisternal spaces; and, hepatocytes arranged around bile canaliculi with small, normal biliary epithelial cells. In addition, the space of Disse was narrow and sinusoids contained abundant red blood cells; mitochondria were numerous, oval shaped with normal, irregularly oriented cristae and narrow lumens; secondary lysosomes were rare and small, and lipid vacuoles were moderately sized and few. Glycogen was present in small deposits toward the periphery of hepatocytes.

The liver from the PETG group was very similar to control. The only difference was an increase in glycogen (Fig. 5B). The AgNO$_3$ exposure group also had increased amounts of glycogen in their livers and portions of RER had transformed into myelin-like bodies (Fig. 5C). We did not observe nanoparticles within the liver from fish exposed to AgNPs. However, when not in large aggregates, their size, shape, and electron density can be similar to granules within glycogen deposits. It is possible that some of these granules were actually AgNPs. Livers from the AgNP treatment group were the most altered. While hepatocytes had increased amounts of glycogen similar to that observed in fish exposed to PETG or AgNO$_3$, the deposits had wide, clear spaces between glycogen granules (Fig. 5D). In addition, plasma membranes and intercellular spaces were indistinct (Fig. 5D), indicating hepatocellular swelling. Lipid vesicles were also abundant and large throughout these cells (Fig. 5D). 2% composite exposure did not result in hepatocellular or biliary change apart from additional glycogen (Fig. 5E). However, macrophages were observed adjacent to biliary and sinusoidal spaces (Fig. 5E). Liver from the 0.5% composite treatment (Fig. 5F) was most similar to that of the liver from the PETG treatment, showing only increased glycogen (Fig. 5F).

4. Discussion

Our study is the first to evaluate toxicity resulting from thermoplastics embedded with AgNPs in a vertebrate. The benefits and risks associated with the use of AgNPs in various fields have been studied for decades.[68] More recently, the number of studies on the impacts of MPs has surged due to increased interest from regulatory agencies, non-profit organizations, and the public among others. As such, the potential adverse impacts of MPs on humans and organisms the environment is becoming better characterized.[69,70] These effects may occur through the plastics, chemicals internally incorporated in them, and/or materials sorbed to their surface during their lifecycle.[71–73] However, exposure risks associated with the generation of silver-containing nanocomposites has not been well studied despite the incorporation of AgNPs into many industrial and consumer products, including plastics. In addition, the oral exposure route is poorly understood.[74] The transparent medaka strain proved a useful tool for the comparison of responses in individuals at multiple levels of biological organization and provided insights into potential risks of oral exposure to AgNP nanocomposites in humans.[45,75]

Tissues composing the gut are both the first line of defense and potentially the most directly impacted by oral exposure. Histology showed AgNO$_3$ and pristine AgNPs to cause changes in these tissues. AgNPs are known to cross biological membranes such as the gut wall and distribute to multiple organs.[28,76,77] Macromolecules and nanoparticles are taken up by the gut epithelium via endocytosis and transported to macrophages in the lamina propria and into circulation[78] For example, Scown et al.[79] demonstrated that increased concentrations of silver in the liver were likely the result of uptake by gut epithelium during exposure to 10 μg L^{-1} to 100 μg L^{-1} AgNPs (49 and 65 nm, unspecified coating). Likewise, high concentrations of silver in the intestine as well as liver and bile of common carp (Cyprinus carpio) were found following aqueous exposure to 0.01 μg L^{-1} and 0.01 μg L^{-1} AgNPs (35 nm, unspecified coating).[80] As fish gut anatomy and function are comparable to that of humans,[81] this suggests similar uptake may occur as a result of analogous exposures to silver in humans. A study of observed an increase in goblet cell density in adult zebrafish exposed to chitosan AgNP nanocomposites via diet for 30 and 60 days.[82] This is the only other study of gut morphologic changes in fish following AgNP nanocomposite exposure.

Studies suggest that the kidney is one of the major sites for nanoparticle accumulation and adverse effects following oral exposure.[77,83,84] We observed a variety of changes in head kidneys, mostly adjacent to large blood vessels that suggested injurious components systemically carried by blood. Tubular epithelial cells were affected in all test groups except controls and were notably one of the few changes observed in fish exposed to PETG. Cell damage and tubular necrosis is a common type of xenobiotic-induced kidney damage in teleosts as there is a high capacity for membrane transport in these cells as well as concentration of compounds in the tubule lumen.[85] In a dietary AgNP exposure in adult zebrafish, Yazdanparast et al.[86] reported similar findings including damage to kidney cells and

This journal is © The Royal Society of Chemistry 2024

Environ. Sci.: Nano, 2024, 11, 3317–3334 | 3327

increased Bowman's space. Flattening or fusion of the pedicels within Bowman's space was an unusual finding unique to fish exposed to nanocomposites in our study. Podocytes with swollen and elongated pedicels have been reported in male rats following intraperitoneal injection of AgNPs (2000 mg kg^{-1}; 20 nm to 65 nm, unspecified coating).[87] This change could have reduced filtration area and hydraulic permeability[85] and may have been linked to the congestion of glomerular capillaries observed in fish in our study. Such reductions in glomerular filtration rate (GFR) and plasma flow are also signs of malnutrition. These renal changes can also result from perturbations in transmembrane signaling transduction,[88] which may have occurred from silver interacting with cell membranes.[89] Boudreau *et al.*[77] reported significant concentrations of silver in kidneys of rats exposed *via* oral gavage to AgNPs, higher even than the Ag$^+$ control (as AgOAc). Within the kidney, they found AgNPs to remain intact and localize to renal tubular epithelium while AgOAc silver granules localized to basement membranes of glomeruli. This is in line with the results of our study. Nanocomposites have been used as therapies to address kidney injury and dysfunction. However, to date, there are no reports for kidney injury resulting from AgNP nanocomposite exposure.

We observed substantial changes to the liver, consistent with reports in both mammals and fish for AgNP accumulation and resultant damage. The liver has been shown to be a site of bioconcentration of AgNPs in both adult medaka[90] and zebrafish,[91] and it is the most likely route of nanomaterial excretion.[92] When adult zebrafish were exposed to aqueous AgNPs (25 nm, unspecified coating, 23.7 µg L^{-1} to 331.8 µg L^{-1}) for 14 days, hepatic parenchyma was less homogenous, with cells in loose contact or irregular in shape.[93] Livers of Siberian sturgeon (*Acipenser baerii*) exposed to aqueous AgNPs (8 nm, unspecified coating, 100 µg L^{-1} to 1500 µg L^{-1}) for 21 days developed dilations and blood congestion in vessels as well as hepatocyte shrinkage and enlargement.[94] Vacuolated hepatocytes and necrotic foci were also reported following dietary exposure of AgNPs (5 nm, PVP/PEI coating, 100 ng L^{-1} and 100 µg L^{-1}) *via Artemia* in zebrafish.[62] When Wu and Zhou[95] exposed adult medaka to aqueous AgNPs (30 nm, PVP coated, 0.05 mg L^{-1} to 0.5 mg L^{-1}) for 14 days, they found congested blood vessels, enlarged hepatocytes, dilation of sinusoidal space, focal necrosis, focal inflammation, and areas of vacuolation in the liver. These findings correspond with what we observed in fish exposed to silver, either pristine or composite. However, it is worthy of mention that some of these studies lack a Ag$^+$ treatment group, so it is unclear if their findings were the result of the nanoparticle or Ag$^+$. There are also no AgNP nanocomposite studies that focus on liver morphology that we can compare to our findings.

We observed hepatocellular alterations in most or all fish in treatment groups containing silver. It was interesting that hepatocellular shrinkage was only observed in fish exposed to nanocomposite materials, specifically near the porta hepatis. It is also noteworthy that we also observed shrunken hepatocytes in our recent study of oral exposure to MWCNT-embedded nanocomposites.[55] This morphology can be indicative of nutrient deprivation,[96] and it can be a symptom of cytoplasmic alterations and aggregation of organelles and is characteristic sign of apoptotic cell death.[97] Importantly, the fish in the control and PETG groups in our study were fasted for the same amounts of time as those in other groups, and this change was not observed, suggesting that the composites were the agent of this change. Conversely, necrotic hepatocytes occurred with exposure to AgNPs but not nanocomposites, suggesting there may be a threshold concentration of AgNPs released from composites to cause this type of significant change. This is a possibility as AgNPs can have strong interactions with their polymer matrices.[14] There is evidence *in vitro* from rainbow trout (*Oncorhynchus mykiss*) hepatocytes that AgNPs inhibit cellular metabolic activity, reduce membrane integrity, and increase reactive oxygen species (ROS) in a dose-dependent manner.[98] Swollen hepatocytes with clear or lightly staining cytoplasm in histologic sections is indicative of glycogen accumulation but cannot be confirmed by H&E staining alone.[88] This is where analyses of multiple levels of biological organization proved valuable. TEM provided confirmation of glycogen accumulation, showing large areas of glycogen in hepatocytes of exposed fish. In teleosts, hepatic intracellular glucose is channeled into glycogen and becomes a major store of carbohydrates.[99] Increased glycogen such as that in fish in our study is a metabolic situation typically associated with food deprivation,[99] and supported our findings in kidney and liver tissues.

Also prevalent in fish of our study was widespread immunological responses. There are a number of studies of toxicant-induced immunotoxicity, but the mechanisms underlying changes are not well understood.[100] In our study, inflammation appeared to be the result of AgNP exposure, both in its pristine form as well as that released from nanocomposites. Many metals are known to be immunotoxic, typically in the disruption of ion influx or reactive oxygen formation.[101] AgNPs can penetrate the serosal layer of the gut and activate serosal macrophages located in the peritoneal cavity[101] as suggested by the macrophages we observed in these areas in histologic sections. Once inside macrophages, lysosomal fluid can increase the amount of silver content on the nanoparticle surface and increase the rate of Ag$^+$ production from AgNPs, a contributor to metallic cytotoxicity.[76] Additionally, lysosomal membrane potential (LMP) is accompanied by the release of cathepsin B, initiating NLRP3 inflammasome assembly and caspase-1 activation.[102] This process leads to the maturation of IL-1β and IL-18 and a subsequent inflammatory response.[102] The ability of AgNPs to initiate this inflammatory pathway *via* LMP has been demonstrated in human liver[103] and lung cells[104] as well as oyster (*Crassostrea virginica*) hepatopancreas tissues.[105]

3328 | *Environ. Sci.: Nano*, 2024, **11**, 3317–3334

This journal is © The Royal Society of Chemistry 2024

Accumulation of white blood cells are indicative of sites of inflammation, reactive oxygen formation, and lipid oxidation.[101] The adaptive immune system in fish shows a slower response than that of mammals, sometimes taking weeks instead of days. *In vitro* studies have shown AgNPs to induce an inflammatory response of which an early stage is the cellular secretion of pro-inflammatory cytokines.[106] It is possible that the inflammation that we observed was in the early stages and a more chronic exposure may be necessary to determine full effects of AgNPs on the immune system. Future investigations should include testing of humoral elements, as well as gene alterations for cell regulation, classes of inflammatory and stress responses.[106]

Considering the commonalities in toxicity of AgNPs across diverse biological systems, cross-species extrapolations may be possible.[80] AgNPs have been shown to distribute, accumulate, and affect more organs compared to other types of nanoparticles, such as gold nanoparticles (*e.g.*, Yang *et al.*[107]). AgNPs are added to various matrices (*e.g.*, polymers) so that their release provides bactericidal and bacteriostatic effects.[108] This incorporation has been viewed as a way to reduce silver toxicity to humans while still imparting antimicrobial benefits.[109] But to date, abrasion studies such as we have conducted have not been done to support this statement. The observations made in our study showed that exposure to pristine AgNPs resulted in the most morphological change as did $AgNO_3$, although to a lesser extent. This suggests that silver is more toxic as a nanoparticle rather than AgNPs being a delivery mechanism for Ag^+. This was supported by our dissolution data, which showed that while dissolution increased slightly over the course of 24 hours for AgNPs, the concentration of dissolved silver did not reach that of equivalent $AgNO_3$. Additionally, the material matrix of the nanocomposites protected from total AgNP or Ag^+ release. Interestingly, the different responses we observed in nanocomposite exposure groups indicate that these advanced materials should be viewed as unique mixtures that may alter the toxic effects of the silvers particles incorporated on the material matrix.

5. Conclusion

Our study is the first to evaluate morphologic changes in a vertebrate resulting from oral exposure to abraded AgNP nanocomposites, a unique mixture of nanoparticles and a plastic polymer. AgNPs and AgNP composites affected a wide range of organs and prompted an immune response. These systemic responses indicate that ingested silver was able to penetrate the gut wall and distribute throughout the body. Effects in both the kidney and liver suggested much of this distribution occurred through the bloodstream. While very few effects were observed with the PETG matrix alone, this component of nanocomposites should not be disregarded as it may have impacted other mechanisms (*e.g.*, microbiome,[110] reproduction[111]). While effects of nanocomposites containing higher loads of AgNPs were

most similar to exposures with pristine AgNPs, we also observed nanocomposites caused different morphological changes within some tissues suggesting unique mixture effects.

Data availability statement

Data that support the findings of this study are available at **https://figshare.com** at **https://doi.org/10.6084/m9.figshare.26042230**. Additional data and figures supporting this article have been included as part of the ESI.†

Conflicts of interest

The authors declare that they have no known competing financial interests or personal relationships that could have appeared to influence the work reported in this paper.

Acknowledgements

References

1 A. Kennedy, J. Brame, T. Rycroft, M. Wood, V. Zemba, C. Weiss Jr., M. Hull, C. Hill, C. Geraci and I. Linkov, A definition and categorization system for advanced materials: The foundation for risk-informed environmental health and safety testing, *Risk Anal.*, 2019, **39**, 1783–1795.

This journal is © The Royal Society of Chemistry 2024

Environ. Sci.: Nano, 2024, **11**, 3317–3334 | **3329**

2   S. Berkner, K. Schwirn and D. Voelker, Too advanced for assessment? Advanced materials, nanomedicine and the environment, *Environ. Sci. Eur.*, 2022, **34**, 71.

3   N. Karak, in *Nanomaterials and Polymer Nanocomposites*, ed. N. Karak, Elsevier, 2019, pp. 1–45, DOI: **10.1016/B978-0-12-814615-6.00001-1**.

4   I. Pacheco and C. Buzea, in *Handbook of Nanomaterials and Nanocomposites for Energy and Environmental Applications*, ed. O. V. Kharissova, L. M. Torres-Martínez and B. I. Kharisov, Springer International Publishing, Cham, 2021, ch. 1, pp. 3–39, DOI: **10.1007/978-3-030-36268-3_1**.

5   V. Ojijo and S. Sinha Ray, in *Processing of Polymer-based Nanocomposites*, ed. S. Sinha Ray, Springer International Publishing, Cham, 2018, pp. 1–14, DOI: **10.1007/978-3-319-97779-9_1**.

6   C. O'Connor, C. Barnes, L. Kent and D. Hammond, *In-depth lab report: design and evaluation of low cost, custom, retrofitted engineering controls for 3D printing*, Department of Health and Human Services, Public Health Service, Centers for Disease Control and Prevention, National Institute for Occupational Safety and Health (NIOSH), Cincinnati, OH, 2022, p. 26.

7   F. L. Chan, R. House, I. Kudla, J. C. Lipszyc, N. Rajaram and S. M. Tarlo, Health survey of employees regularly using 3D printers, *Occup. Med.*, 2018, **68**, 211–214.

8   W. C. Hill, D. W. Seitz, M. S. Hull, M. L. Ballentine and A. J. Kennedy, Additives influence 3D printer emission profiles: Implications for working safely with polymer filament composites, *Indoor Air*, 2022, **32**, e13130.

9   E. Alberts, M. Ballentine, E. Barnes and A. Kennedy, Impact of metal additives on particle emission profiles from a fused filament fabrication 3D printer, *Atmos. Environ.*, 2021, **244**, 117956.

10 J. Pelley, Safety Standards Aim to Rein in 3-D Printer Emissions, *ACS Cent. Sci.*, 2018, **4**, 134–136.

11 E. Glassford, K. L. Dunn, K. H. Dunn, D. Hammond and J. Tyrawski, in *Health Effects from Exposures To 3D Printer Emissions*, ed. NIOSH, Department of Health and Human Services, Centers for Disease Control and Prevention, National Institute for Occupational Safety and Health, DHHS (NIOSH), Cincinnati, OH, 2020, p. 1.

12 C. Buzea, I. I. Pacheco and K. Robbie, Nanomaterials and nanoparticles: Sources and toxicity, *Biointerphases*, 2007, **2**, MR17–MR71.

13 N. Barrera, L. Guerrero, A. Debut and P. Santa-Cruz, Printable nanocomposites of polymers and silver nanoparticles for antibacterial devices produced by DoD technology, *PLoS One*, 2018, **13**, e0200918.

14 N. Karak, in *Nanomaterials and Polymer Nanocomposites*, ed. N. Karak, Elsevier, 2019, ch. 2, pp. 47–89, DOI: **10.1016/B978-0-12-814615-6.00002-3**.

15 P. Dallas, V. K. Sharma and R. Zboril, Silver polymeric nanocomposites as advanced antimicrobial agents: classification, synthetic paths, applications, and perspectives, *Adv. Colloid Interface Sci.*, 2011, **166**, 119–135.

16 A. Hazra Chowdhury, R. Debnath, S. Manirul Islam and T. Saha, in *Sustainable Polymer Composites and Nanocomposites*, ed. I.-S. Thomas, R. Kumar Mishra and A. M. Asiri, Springer International Publishing, Cham, 2019, ch. 37, pp. 1067–1091, DOI: **10.1007/978-3-030-05399-4_37**.

17 S. Silver, Bacterial silver resistance: molecular biology and uses and misuses of silver compounds, *FEMS Microbiol. Rev.*, 2003, **27**, 341–353.

18 S. S. Ahmad, O. Yousuf, R. U. Islam and K. Younis, Silver nanoparticles as an active packaging ingredient and its toxicity, *Packag. Technol. Sci.*, 2021, **34**, 653–663.

19 Z. Ferdous and A. Nemmar, Health impact of silver nanoparticles: A review of the biodistribution and toxicity following various routes of exposure, *Int. J. Mol. Sci.*, 2020, **21**, 2375.

20 T. Yang, T. Paulose, B. W. Redan, J. C. Mabon and T. V. Duncan, Food and beverage ingredients induce the formation of silver nanoparticles in products stored within nanotechnology-enabled packaging, *ACS Appl. Mater. Interfaces*, 2021, **13**, 1398–1412.

21 T. V. Duncan and K. Pillai, Release of engineered nanomaterials from polymer nanocomposites: Diffusion, dissolution, and desorption, *ACS Appl. Mater. Interfaces*, 2015, **7**, 2–19.

22 E. O. Simbine, L. D. C. Rodrigues, J. Lapa-Guimaraes, E. S. Kamimura, C. H. Corassin and C. A. F. de Oliveira, Application of silver nanoparticles in food packages: a review, *Food Sci. Technol.*, 2019, **39**, 793–802.

23 M. E. Quadros, R. Pierson, N. S. Tulve, R. Willis, K. Rogers, T. A. Thomas and L. C. Marr, Release of silver from nanotechnology-based consumer products for children, *Environ. Sci. Technol.*, 2013, **47**, 8894–8901.

24 T. Benn, B. Cavanagh, K. Hristovski, J. D. Posner and P. Westerhoff, The release of nanosilver from consumer products used in the home, *J. Environ. Qual.*, 2010, **39**, 1875–1882.

25 Z. Ouyang, Z. Mao, R. Hu, E. Hu, C. Xiao, C. Yang and X. Guo, The indoor exposure of microplastics in different environments, *Gondwana Res.*, 2022, **108**, 193–199.

26 Y. Jiang, J. Han, J. Na, J. Fang, C. Qi, J. Lu, X. Liu, C. Zhou, J. Feng, W. Zhu, L. Liu, H. Jiang, Z. Hua, G. Pan, L. Yan, W. Sun and Z. Yang, Exposure to microplastics in the upper respiratory tract of indoor and outdoor workers, *Chemosphere*, 2022, **307**, 136067.

27 K. M. Kleinow and M. O. James, in *Target Organ Toxicity in Marine and Freshwater Teleosts*, ed. D. Schlenk and W. H. Benson, CRC Press, Boca Raton, FL, 2001, ch. 5, vol. 1, pp. 269–362.

28 J. G. Coleman, A. J. Kennedy, A. J. Bednar, J. F. Ranville, J. G. Laird, A. R. Harmon, C. A. Hayes, E. P. Gray, C. P. Higgins, G. Lotufo and J. A. Steevens, Comparing the effects of nanosilver size and coating variations on bioavailability, internalization, and elimination, using Lumbriculus variegatus, *Environ. Toxicol. Chem.*, 2013, **32**, 2069–2077.

29 J. Fabrega, S. N. Luoma, C. R. Tyler, T. S. Galloway and J. R. Lead, Silver nanoparticles: behaviour and effects in the aquatic environment, *Environ. Int.*, 2011, **37**, 517–531.

30 K. W. H. Kwok, M. Auffan, A. R. Badireddy, C. M. Nelson, M. R. Wiesner, A. Chilkoti, J. Liu, S. M. Marinakos and D. E. Hinton, Uptake of silver nanoparticles and toxicity to

3330 | *Environ. Sci.: Nano*, 2024, **11**, 3317–3334

This journal is © The Royal Society of Chemistry 2024

early life stages of Japanese medaka (Oryzias latipes): effect of coating materials, *Aquat. Toxicol.*, 2012, **120**, 59–66.

31 J. M. Lacave, U. Vicario-Parés, E. Bilbao, D. Gilliland, F. Mura, L. Dini, M. P. Cajaraville and A. Orbea, Waterborne exposure of adult zebrafish to silver nanoparticles and to ionic silver results in differential silver accumulation and effects at cellular and molecular levels, *Sci. Total Environ.*, 2018, **642**, 1209–1220.

32 A. Bermejo-Nogales, M. Fernández, M. L. Fernández-Cruz and J. M. Navas, Effects of a silver nanomaterial on cellular organelles and time course of oxidative stress in a fish cell line (PLHC-1), *Comp. Biochem. Physiol., Part C: Toxicol. Pharmacol.*, 2016, **190**, 54–65.

33 M. S. A. Darwish, M. H. Mostafa and L. M. Al-Harbi, Polymeric nanocomposites for environmental and industrial applications, *Int. J. Mol. Sci.*, 2022, **23**, 1023.

34 ERDC, Environmental Risk Assessment: Advance Materials, Tools and Resources, **https://nano.el.erdc.dren.mil/tools.html**, 2021).

35 L. T. Haber, A. J. Bednar, A. J. Kennedy, M. L. Ballentine and R. A. Canady, *Methods Evaluation for Assessing Release of Manufactured Nanomaterials from Polymers, Consistent with the NanoGRID Framework: Advanced and Additive Materials: Sustainability for Army Acquisitions*, Army Engineer Research and Development Center, Vicksburg United States, 2019.

36 P. Byrley, B. J. George, W. K. Boyes and K. Rogers, Particle emissions from fused deposition modeling 3D printers: Evaluation and meta-analysis, *Sci. Total Environ.*, 2019, **655**, 395–407.

37 N. Bossa, J. M. Sipe, W. Berger, K. Scott, A. J. Kennedy, T. Thomas, C. O. Hendren and M. R. Wiesner, Quantifying mechanical abrasion of MWCNT nanocomposites used in 3D printing: Influence of CNT content on abrasion products and rate of microplastic production, *Environ. Sci. Technol.*, 2021, **55**, 10332–10342.

38 K. Szykiedans, W. Credo and D. Osiński, Selected mechanical properties of PETG 3-D prints, *Xxi Polish-Slovak Scientific Conference Machine Modeling and Simulations Mms*, 2017, vol. 177, pp. 455–461.

39 G. Dolzyk and S. Jung, Tensile and fatigue analysis of 3D-printed polyethylene terephthalate glycol, *J. Fail. Anal. Prev.*, 2019, **19**, 511–518.

40 J. C. Prata, J. P. da Costa, I. Lopes, A. C. Duarte and T. Rocha-Santos, Environmental exposure to microplastics: An overview on possible human health effects, *Sci. Total Environ.*, 2020, **702**, 134455.

41 C. Pedà, L. Caccamo, M. C. Fossi, F. Gai, F. Andaloro, L. Genovese, A. Perdichizzi, T. Romeo and G. Maricchiolo, Intestinal alterations in European sea bass Dicentrarchus labrax (Linnaeus, 1758) exposed to microplastics: Preliminary results, *Environ. Pollut.*, 2016, **212**, 251–256.

42 H. Gu, S. Wang, X. Wang, X. Yu, M. Hu, W. Huang and Y. Wang, Nanoplastics impair the intestinal health of the juvenile large yellow croaker Larimichthys crocea, *J. Hazard. Mater.*, 2020, **397**, 122773.

43 M. Zhu, M. Chernick, D. Rittschof and D. E. Hinton, Chronic dietary exposure to polystyrene microplastics in maturing Japanese medaka (Oryzias latipes), *Aquat. Toxicol.*, 2020, **220**, 105396.

44 A. M. Lopes, H.-U. Dahms, A. Converti and G. L. Mariottini, Role of model organisms and nanocompounds in human health risk assessment, *Environ. Monit. Assess.*, 2021, **193**, 285.

45 A. Planchart, C. J. Mattingly, D. Allen, P. Ceger, W. Casey, D. Hinton, J. Kanungo, S. W. Kullman, T. Tal, M. Bondesson, S. M. Burgess, C. Sullivan, C. Kim, M. Behl, S. Padilla, D. M. Reif, R. L. Tanguay and J. Hamm, Advancing toxicology research using in vivo high throughput toxicology with small fish models, *ALTEX*, 2016, **33**, 435–452.

46 K. Dooley and L. I. Zon, Zebrafish: a model system for the study of human disease, *Curr. Opin. Genet. Dev.*, 2000, **10**, 252–256.

47 R. B. Walter and T. Obara, Workshop report: The medaka model for comparative assessment of human disease mechanisms, Comparative biochemistry and physiology, *Toxicology & pharmacology : CBP*, 2015, **178**, 156–162.

48 N. Aghaallaei, F. Gruhl, C. Q. Schaefer, T. Wernet, V. Weinhardt, L. Centanin, F. Loosli, T. Baumbach and J. Wittbrodt, Identification, visualization and clonal analysis of intestinal stem cells in fish, *Development*, 2016, **143**, 3470–3480.

49 S. Brugman, The zebrafish as a model to study intestinal inflammation, *Dev. Comp. Immunol.*, 2016, **64**, 82–92.

50 X. Zhao and M. Pack, in *Methods in Cell Biology*, ed. H. W. Detrich, M. Westerfield and L. I. Zon, Academic Press, Cambridge, MA, 2017, vol. 138, pp. 241–270.

51 J. M. Sipe, W. Berger, N. Bossa, M. Chernick, K. Scott, A. Kennedy, T. Thomas, C. O. Hendren and M. R. Wiesner, Quantifying mechanical abrasion of AgNP Nanocomposites used in 3D Printing: Influence of AgNP content on abrasion products and rate of microplastic production, *Environ. Sci.: Nano*, 2024, DOI: **10.1039/D3EN00888F**.

52 D. E. Hinton and J. A. Couch, in *Fish Ecotoxicology*, ed. T. Braunbeck, D. E. Hinton and B. Streit, Birkhauser Verlag, Basel, Switzerland, 1998, pp. 141–164.

53 S. Bao, W. Tang and T. Fang, Sex-dependent and organ-specific toxicity of silver nanoparticles in livers and intestines of adult zebrafish, *Chemosphere*, 2020, **249**, 126172.

54 Y. Lu, Y. Zhang, Y. Deng, W. Jiang, Y. Zhao, J. Geng, L. Ding and H. Ren, Uptake and accumulation of polystyrene microplastics in zebrafish (Danio rerio) and toxic effects in liver, *Environ. Sci. Technol.*, 2016, **50**, 4054–4060.

55 M. Chernick, A. J. Kennedy, T. Thomas, K. C. K. Scott, C. O. Hendren, M. R. Wiesner and D. E. Hinton, Impacts of ingested MWCNT-Embedded nanocomposites in Japanese medaka (Oryzias latipes), *Nanotoxicology*, 2021, **15**, 1403–1422.

56 J. M. Sipe, N. Bossa, W. Berger, N. von Windheim, K. Gall and M. R. Wiesner, From bottle to microplastics: Can we

This journal is © The Royal Society of Chemistry 2024

Environ. Sci.: Nano, 2024, **11**, 3317–3334 | **3331**

estimate how our plastic products are breaking down?, *Sci. Total Environ.*, 2022, **814**, 152460.

57 K. C. K. Scott, M. R. Wiesner, J. M. Sipe and N. Bossa, Correlating mechanical abrasion with power input, *NIST Spec. Publ.*, 2022, **1200**, 30.

58 I. Fernando and Y. Zhou, Impact of pH on the stability, dissolution and aggregation kinetics of silver nanoparticles, *Chemosphere*, 2019, **216**, 297–305.

59 J. M. Wilson and L. F. C. Castro, in *Fish Physiology*, ed. M. Grosell, A. P. Farrell and C. J. Brauner, Academic Press, New York, NY, 2010, vol. 30, pp. 1–55.

60 M. K. Hamilton, E. S. Wall, C. D. Robinson, K. Guillemin and J. S. Eisen, Enteric nervous system modulation of luminal pH modifies the microbial environment to promote intestinal health, *PLoS Pathog.*, 2022, **18**, e1009989.

61 T. Sasado, M. Tanaka, K. Kobayashi, T. Sato, M. Sakaizumi and K. Naruse, Quintet Strain Information, **https://shigen. nig.ac.jp/medaka/strainDetailAction.do?strainId=467**, (accessed 11/28/2018, 2018).

62 J. M. Lacave, Á. Fanjul, E. Bilbao, N. Gutierrez, I. Barrio, I. Arostegui, M. P. Cajaraville and A. Orbea, Acute toxicity, bioaccumulation and effects of dietary transfer of silver from brine shrimp exposed to PVP/PEI-coated silver nanoparticles to zebrafish, Comparative biochemistry and physiology, *Toxicology & pharmacology: CBP*, 2017, **199**, 69–80.

63 D. L. Merrifield, B. J. Shaw, G. M. Harper, I. P. Saoud, S. J. Davies, R. D. Handy and T. B. Henry, Ingestion of metal-nanoparticle contaminated food disrupts endogenous microbiota in zebrafish (Danio rerio), *Environ. Pollut.*, 2013, **174**, 157–163.

64 J. Wang and W.-X. Wang, Low bioavailability of silver nanoparticles presents trophic toxicity to marine medaka (Oryzias melastigma), *Environ. Sci. Technol.*, 2014, **48**, 8152–8161.

65 Z. Chen, X. Sheng, J. Wang and Y. Wen, Silver nanoparticles or free silver ions work? An enantioselective phytotoxicity study with a chiral tool, *Sci. Total Environ.*, 2018, **610-611**, 77–83.

66 J. Liu and R. H. Hurt, Ion release kinetics and particle persistence in aqueous nano-silver colloids, *Environ. Sci. Technol.*, 2010, **44**, 2169–2175.

67 C. Levard, E. M. Hotze, G. V. Lowry and G. E. Brown, Jr., Environmental transformations of silver nanoparticles: impact on stability and toxicity, *Environ. Sci. Technol.*, 2012, **46**, 6900–6914.

68 S. W. P. Wijnhoven, W. J. G. M. Peijnenburg, C. A. Herberts, W. I. Hagens, A. G. Oomen, E. H. W. Heugens, B. Roszek, J. Bisschops, I. Gosens, D. Van de Meent, S. Dekkers, W. H. De Jong, M. Van Zijverden, A. J. A. M. Sips and R. E. Geertsma, Nano-silver - A review of available data and knowledge gaps in human and environmental risk assessment, *Nanotoxicology*, 2009, **3**, 109–178.

69 S. Kacprzak and L. D. Tijing, Microplastics in indoor environment: Sources, mitigation and fate, *J. Environ. Chem. Eng.*, 2022, **10**, 107359.

70 M. D. Prokic, B. R. Gavrilovic, T. B. Radovanovic, J. P. Gavric, T. G. Petrovic, S. G. Despotovic and C. Faggio, Studying microplastics: Lessons from evaluated literature on animal model organisms and experimental approaches, *J. Hazard. Mater.*, 2021, **414**, 125476.

71 M. D. Prokić, T. B. Radovanović, J. P. Gavrić and C. Faggio, Ecotoxicological effects of microplastics: Examination of biomarkers, current state and future perspectives, *TrAC, Trends Anal. Chem.*, 2019, **111**, 37–46.

72 J. H. Bridson, E. C. Gaugler, D. A. Smith, G. L. Northcott and S. Gaw, Leaching and extraction of additives from plastic pollution to inform environmental risk: A multidisciplinary review of analytical approaches, *J. Hazard. Mater.*, 2021, **414**, 125571.

73 X. Cousin, A. Batel, A. Bringer, S. Hess, M.-L. Bégout and T. Braunbeck, Microplastics and sorbed contaminants – Trophic exposure in fish sensitive early life stages, *Mar. Environ. Res.*, 2020, 105126, DOI: **10.1016/j. marenvres.2020.105126**.

74 I. Zorraquín-Peña, C. Cueva, B. Bartolomé and M. V. Moreno-Arribas, Silver nanoparticles against foodborne bacteria. Effects at intestinal level and health limitations, *Microorganisms*, 2020, **8**, 132.

75 Y. Wakamatsu, S. Pristyazhnyuk, M. Kinoshita, M. Tanaka and K. Ozato, The see-through medaka: A fish model that is transparent throughout life, *Proc. Natl. Acad. Sci.*, 2001, **98**, 10046–10050.

76 L. K. Braydich-Stolle, E. K. Breitner, K. K. Comfort, J. J. Schlager and S. M. Hussain, Dynamic characteristics of silver nanoparticles in physiological fluids: Toxicological implications, *Langmuir*, 2014, **30**, 15309–15316.

77 M. D. Boudreau, M. S. Imam, A. M. Paredes, M. S. Bryant, C. K. Cunningham, R. P. Felton, M. Y. Jones, K. J. Davis and G. R. Olson, Differential effects of silver nanoparticles and silver ions on tissue accumulation, distribution, and toxicity in the Sprague Dawley rat following daily oral gavage administration for 13 weeks, *Toxicol. Sci.*, 2016, **150**, 131–160.

78 C. M. Press and Ø. Evensen, The morphology of the immune system in teleost fishes, *Fish Shellfish Immunol.*, 1999, **9**, 309–318.

79 T. M. Scown, E. M. Santos, B. D. Johnston, B. Gaiser, M. Baalousha, S. Mitov, J. R. Lead, V. Stone, T. F. Fernandes, M. Jepson, R. van Aerle and C. R. Tyler, Effects of aqueous exposure to silver nanoparticles of different sizes in rainbow trout, *Toxicol. Sci.*, 2010, **115**, 521–534.

80 B. K. Gaiser, T. F. Fernandes, M. A. Jepson, J. R. Lead, C. R. Tyler, M. Baalousha, A. Biswas, G. J. Britton, P. A. Cole, B. D. Johnston, Y. Ju-Nam, P. Rosenkranz, T. M. Scown and V. Stone, Interspecies comparisons on the uptake and toxicity of silver and cerium dioxide nanoparticles, *Environ. Toxicol. Chem.*, 2012, **31**, 144–154.

81 K. N. Wallace, S. Akhter, E. M. Smith, K. Lorent and M. Pack, Intestinal growth and differentiation in zebrafish, *Mech. Dev.*, 2005, **122**, 157–173.

3332 | *Environ. Sci.: Nano*, 2024, **11**, 3317–3334

This journal is © The Royal Society of Chemistry 2024

82 R. M. C. Udayangani, S. H. S. Dananjaya, C. Nikapitiya, G.-J. Heo, J. Lee and M. De Zoysa, Metagenomics analysis of gut microbiota and immune modulation in zebrafish (Danio rerio) fed chitosan silver nanocomposites, *Fish Shellfish Immunol.*, 2017, **66**, 173–184.

83 S. B. Vasanth and G. A. Kurian, Toxicity evaluation of silver nanoparticles synthesized by chemical and green route in different experimental models, *Artif. Cells, Nanomed., Biotechnol.*, 2017, **45**, 1721–1727.

84 S. V. S. Rana, Recent advances on renal toxicity of engineered nanoparticles—a review, *IJTRA*, 2021, **7**, 036.

85 B. K. Larsen and E. J. Perkins, in *Target Organ Toxicity in Marine and Freshwater Teleosts*, ed. D. Schlenk and W. H. Benson, CRC Press, Boca Raton, FL, 2001, ch. 2, vol. 1, pp. 90–150.

86 T. Yazdanparast, I. Sharifpour, M. Soltani and H. K. Esfahani, Evaluation of silver retention in different organs of zebrafish (Danio rerio) fed diet supplemented with silver nanoparticles, *Int. J. Engine Res.*, 2016, **5**, 269–274.

87 O. M. M. Sarhan and R. M. Hussein, Effects of intraperitoneally injected silver nanoparticles on histological structures and blood parameters in the albino rat, *Int. J. Nanomed.*, 2014, **9**, 1505–1517.

88 W. M. Haschek, C. G. Rousseaux and M. A. Wallig, *Fundamentals of Toxicologic Pathology*, Academic Press, Burlington, MA, 2nd edn, 2010.

89 R. Tiwari, R. D. Singh, H. Khan, S. Gangopadhyay, S. Mittal, V. Singh, N. Arjaria, J. Shankar, S. K. Roy, D. Singh and V. Srivastava, Oral subchronic exposure to silver nanoparticles causes renal damage through apoptotic impairment and necrotic cell death, *Nanotoxicology*, 2017, **11**, 671–686.

90 Y.-J. Jung, K.-T. Kim, J. Y. Kim, S.-Y. Yang, B.-G. Lee and S. D. Kim, Bioconcentration and distribution of silver nanoparticles in Japanese medaka (Oryzias latipes), *J. Hazard. Mater.*, 2014, **267**, 206–213.

91 J. E. Choi, S. Kim, J. H. Ahn, P. Youn, J. S. Kang, K. Park, J. Yi and D.-Y. Ryu, Induction of oxidative stress and apoptosis by silver nanoparticles in the liver of adult zebrafish, *Aquat. Toxicol.*, 2010, **100**, 151–159.

92 R. D. Handy, G. Al-Bairuty, A. Al-Jubory, C. S. Ramsden, D. Boyle, B. J. Shaw and T. B. Henry, Effects of manufactured nanomaterials on fishes: a target organ and body systems physiology approach, *J. Fish Biol.*, 2011, **79**, 821–853.

93 C. Krishnaraj, S. L. Harper and S.-I. Yun, In vivo toxicological assessment of biologically synthesized silver nanoparticles in adult Zebrafish (Danio rerio), *J. Hazard. Mater.*, 2016, **301**, 480–491.

94 T. Ostaszewska, M. Chojnacki, M. Kamaszewski and E. Sawosz-Chwalibóg, Histopathological effects of silver and copper nanoparticles on the epidermis, gills, and liver of Siberian sturgeon, *Environ. Sci. Pollut. Res.*, 2016, **23**, 1621–1633.

95 Y. Wu and Q. Zhou, Silver nanoparticles cause oxidative damage and histological changes in medaka (Oryzias latipes) after 14 days of exposure, *Environ. Toxicol. Chem.*, 2013, **32**, 165–173.

96 S. Mumford, J. Heidel, C. Smith, J. Morrison, B. MacConnell and V. S. Blazer, *Fish histology and histopathology*, US Fish and Wildlife Service's National Conservation Training Center, Shepherdstown, WV, USA, 2007.

97 C. Benz, S. Angermüller, G. Otto, P. Sauer, W. Stremmel and A. Stiehl, Effect of tauroursodeoxycholic acid on bile acid-induced apoptosis in primary human hepatocytes, *Eur. J. Clin. Invest.*, 2000, **30**, 203–209.

98 J. Farkas, P. Christian, J. A. G. Urrea, N. Roos, M. Hassellöv, K. E. Tollefsen and K. V. Thomas, Effects of silver and gold nanoparticles on rainbow trout (Oncorhynchus mykiss) hepatocytes, *Aquat. Toxicol.*, 2010, **96**, 44–52.

99 D. E. Hinton, H. Segner and T. Braunbeck, in *Target Organ Toxicity in Marine and Freshwater Teleosts*, ed. D. Schlenk and W. H. Benson, Taylor and Francis, London, 2001, vol. 1, pp. 224–268.

100 H. Segner, A. M. Möller, M. Wenger and A. Casanova-Nakayama, in *Interdisciplinary Studies on Environmental Chemistry—Environmental Pollution and Ecotoxicology*, ed. M. Kawaguchi, K. Misaki, H. Sato, T. Yokokawa, T. Itai, T. M. Nguyen, J. Ono and S. Tanabe, TERRAPUB, 2012, pp. 1–12.

101 C. D. Rice, in *Target Organ Toxicity in Marine and Freshwater Teleosts*, ed. D. Schlenk and W. H. Benson, Taylor & Francis, New York, NY, 2001, ch. 3, vol. 2, pp. 96–138.

102 OECD, in *Series on the Safety of Manufactured Nanomaterials, No. 92*, OECD Publishing, Paris, 2020, vol. ENV/JM/MONO(2020)32.

103 A. R. Mishra, J. Zheng, X. Tang and P. L. Goering, Silver nanoparticle-induced autophagic-lysosomal disruption and NLRP3-inflammasome activation in HepG2 cells is size-dependent, *Toxicol. Sci.*, 2016, **150**, 473–487.

104 T. Miyayama and M. Matsuoka, Involvement of lysosomal dysfunction in silver nanoparticle-induced cellular damage in A549 human lung alveolar epithelial cells, *J. Occup. Med. Toxicol.*, 2016, **11**, 1.

105 M. P. McCarthy, D. L. Carroll and A. H. Ringwood, Tissue specific responses of oysters, Crassostrea virginica, to silver nanoparticles, *Aquat. Toxicol.*, 2013, **138–139**, 123–128.

106 K. K. Comfort, L. K. Braydich-Stolle, E. I. Maurer and S. M. Hussain, Less is more: long-term in vitro exposure to low levels of silver nanoparticles provides new insights for nanomaterial evaluation, *ACS Nano*, 2014, **8**, 3260–3271.

107 L. Yang, H. Kuang, W. Zhang, Z. P. Aguilar, H. Wei and H. Xu, Comparisons of the biodistribution and toxicological examinations after repeated intravenous administration of silver and gold nanoparticles in mice, *Sci. Rep.*, 2017, **7**, 3303–3303.

108 L. A. Tamayo, P. A. Zapata, N. D. Vejar, M. I. Azócar, M. A. Gulppi, X. Zhou, G. E. Thompson, F. M. Rabagliati and M. A. Páez, Release of silver and copper nanoparticles from polyethylene nanocomposites and their penetration into Listeria monocytogenes, *Mater. Sci. Eng., C*, 2014, **40**, 24–31.

This journal is © The Royal Society of Chemistry 2024

Environ. Sci.: Nano, 2024, **11**, 3317–3334 | **3333**

109 K. Naik and M. Kowshik, The silver lining: towards the responsible and limited usage of silver, *J. Appl. Microbiol.*, 2017, **123**, 1068–1087.

110 C. Zhang, F. Li, X. Liu, L. Xie, Y. T. Zhang and J. Mu, Polylactic acid (PLA), polyethylene terephthalate (PET), and polystyrene (PS) microplastics differently affect the gut microbiota of marine medaka (Oryzias melastigma) after individual and combined exposure with sulfamethazine, *Aquat. Toxicol.*, 2023, 106522, in press.

111 Y. Cong, F. Jin, M. Tian, J. Wang, H. Shi, Y. Wang and J. Mu, Ingestion, egestion and post-exposure effects of polystyrene microspheres on marine medaka (Oryzias melastigma), *Chemosphere*, 2019, **228**, 93–100.

3334 | *Environ. Sci.: Nano*, 2024, **11**, 3317–3334

This journal is © The Royal Society of Chemistry 2024